

archives
of thermodynamics

Vol. 39(2018), No. 4, 85–111

DOI: 10.1515/aoter-2018-0031

Natural convection heat transfer in heated vertical tubes with internal rings

RAMESH CHANDRA NAYAK^{a,*}
MANMATHA KUMAR ROUL^b
SAROJ KUMAR SARANGI^a

^a Department of Mechanical Engineering, Siksha 'O' Anusandhan University, Bhubaneswar, PIN-751030, India

^b Department of Mechanical Engineering, Gandhi Institute for Technological Advancement, Bhubaneswar, Odisha, PIN-752054, India

Abstract Experimental investigation of natural convection heat transfer in heated vertical tubes dissipating heat from the internal surface is presented. The test section is electrically heated and constant wall heat flux is maintained both circumferentially and axially. Four different test sections are taken having 45 mm internal diameter and 3.8 mm thickness. The length of the test sections are 450 mm, 550 mm, 700 mm and 850 mm. Ratios of length to diameter of the test sections are taken as 10, 12.22, 15.56, and 18.89. Wall heat fluxes are maintained at 250–3341 W/m². Experiments are also conducted on channels with internal rings of rectangular section placed at various distances. Thickness of the rings are taken as 4 mm, 6 mm, and 8 mm. The step size of the rings varies from 75 mm to 283.3 mm. The non-dimensional ring spacing, expressed as the ratios of step size to diameter, are taken from 1.67 to 6.29 and the non-dimensional ring thickness, expressed as the ratios of ring thickness to diameter are taken from 0.089 to 0.178. The ratios of ring spacing to its thickness are taken as 9.375 to 70.82. The effects of various parameters such as length to diameter ratio, wall heat flux, ring thickness and ring spacing on local steady-state heat transfer behavior are observed. From the experimental data a correlation is developed for average Nusselt number and modified Rayleigh number. Another correlation is also developed for modified Rayleigh number and modified Reynolds number. These correlations can predict the data accurately within $\pm 10\%$ error.

*Corresponding Author. Email: rameshnayak23@gmail.com

Keywords: Heat flux; Heat transfer; Natural convection; Ring spacing; Ring thickness

Nomenclature

A	–	surface area of test section, m^2
C	–	constant
D	–	diameter of the cylinder, m
g	–	gravitational acceleration, m/s^2
h	–	heat transfer coefficient, W/m^2K
k	–	thermal conductivity, W/mK
L	–	length of the test sections, length of the surface, m
m	–	constant
q_w	–	uniform surface heat flux, W/m^2
T	–	absolute temperature, K
T_b	–	bulk temperature (the temperature of the fluid that is "far" from the wall), K
T_f	–	film temperature, K
T_w	–	wall temperature, K
T_∞	–	free-stream temperature, K
t	–	thickness of the ring, m
s	–	ring spacing, m
u	–	velocity in the boundary layer, m/s
x	–	characteristic length, m
Ra_x	–	Rayleigh number for characteristic length x
Gr_x	–	Grashof number for characteristic length x
Nu	–	Nusselt number
Nu_L	–	Nusselt number for characteristic length x
Pr	–	Prandtl number
Ra^*	–	modified Rayleigh number

Greek symbols

α	–	thermal diffusivity, m^2/s
β	–	thermal expansion coefficient ($= 1/T$), $1/K$
δ	–	boundary layer thickness
ν	–	kinematic viscosity, $Pa \cdot s$
$\Delta T = T - T_w$	–	difference of temperature between wall and ambient temperature, K

Subscripts

$\overline{(\cdot)}$	–	average value
$(\cdot)^*$	–	modified

1 Introduction

Application of natural convection heat transfer can be observed in many areas of engineering fields, such as solar collectors, environmental engineering

and electronic equipment. This is the common method used in electronics cooling, where a large number of thermal connection modules are accommodated on a small base. This category includes stand-alone packages such as modems and small computers having an array of printed circuit boards (PCB) mounted within an enclosure. As the density of these heat producing modules increases day by day, for more compactness, the heat released should be transferred from the surface not only to protect them but also for longer life. Natural convection is a type of heat transfer, in which the fluid motion is not generated by any external source but only by density differences in the fluid occurring due to temperature gradients. In natural convection, fluid surrounding a heat source receives heat, becomes less dense and rises. The surrounding cooler fluid then moves to replace it. This cooler fluid is then heated and the process continues, forming convection current. The driving force for natural convection is buoyancy which arises as a result of differences in fluid density. Since the fluid velocity associated with natural convection is relatively low, the heat transfer coefficient encountered in natural convection is also low. Natural convection heat transfer depends on the geometry of the surface as well as its orientation. It also depends on the variation of temperature on the surface and the thermophysical properties of the fluid. At present, flow of gaseous heat carriers in vertical channels with natural convection is extensively encountered in science and engineering. For example, its application can be observed in domestic convectors, cooling systems of radio electronic and electrical equipment, nuclear reactors with passive cooling systems, dry cooling towers, ground thermosiphons, etc. In such applications, it is required to cool the internal surfaces of vertical open-ended pipes by natural convection, despite the low rates of heat transfer that this convection process affords. The amount of heat that can be removed from an electronic component that is cooled by natural convection can be substantially increased by increasing the surface area of the components. In recent years, the natural convection heat transfer problem has received increasing attention in the literature due to its wide applications.

Iyi and Hasan [1] studied on natural convection flow and heat transfer in an enclosure containing staggered arrangement of blockages. They found numerical results allow a better understanding on the influence of blockages arrangement within a low turbulent natural convection flow in an enclosure. The influence on fluid flow and heat transfer for the different stacking of arrangement of the blockages within the enclosure was

identified and detailed profiles at the mid-height and mid-width of the rectangular enclosure have been analyzed. Buonomo and Manca [2] numerically investigated the transient natural convection in parallel-plate vertical micro channels. The vertical micro channel is considered asymmetrically or symmetrically heated at uniform heat flux. The first-order model for slip velocity and jump temperature is assumed in microscale conditions. The analysis is performed under laminar boundary layer assumption for different values of Knudsen number, Rayleigh number and the ratio of wall heat flux in order to evaluate their effects on wall temperatures, mass flow rate, velocity profiles and Nusselt number. Mallik and Sastri [3] studied experimentally the natural convection heat transfer over an array of staggered discrete vertical plates and found that the use of discrete vertical plates in lieu of continuous plates gives rise to enhancement of natural convection heat transfer. The highest local heat transfer values are encountered at the leading edge and least at the trailing edge of each plate for a particular temperature level and spacing. The highest value corresponds to the thinnest thermal boundary layer and as the thermal boundary layer starts growing from the leading edge of each plate, the heat transfer values starts decreasing and reach a minimum at the trailing edge. Had the plates been continuous, there would have been decrease in the heat transfer values continuously along the height of the vertical plate for same input conditions. They also found that the heat transfer quantities at the leading edge of the top plate are more than that at the trailing edge but less than that at the leading edge of the bottom plate. Degree of enhancement increases with the increase in spacing.

Huang *et al.* [4] studied overall convective heat transfer coefficients of the perforated fin arrays lying between two limits corresponding to the imperforate fin arrays and vertical parallel plates, respectively. The overall convective heat transfer coefficients of the perforated fin arrays increase with increasing total perforation length. Cheng [5] studied effects of the modified Darcy number, the buoyancy ratio and the inner radius-gap ratio on the fully developed natural convection heat and mass transfer in a vertical annular non-Darcy porous medium with asymmetric wall temperatures and concentrations. The exact solutions for the important characteristics of fluid flow, heat transfer, and mass transfer are derived by using the non-Darcy flow model. The modified Darcy number is related to the flow resistance of the porous matrix. For the free convection heat and mass transfer in the annular duct filled with porous media, increasing the mod-

ified Darcy number tends to increase the volume flow rate, total heat rate added to the fluid, and the total species rate added to the fluid. Moreover, an increase in the buoyancy ratio or in the inner radius-gap ratio leads to the increase in the volume flow rate, the total heat rate added to the fluid, and the total species rate added to the fluid. Capobianchi and Aziz [6] analyzed natural convective flows over vertical surfaces and found that the local Nusselt number is an implicit function of the Biot number characterizing the convective heating on the backside of the plate. The order of magnitude of the local Nusselt number was therefore evaluated numerically for three values each of the Boussinesq, Prandtl, and Biot number.

Experimental study of Sparrow and Bahrami [7] encompasses three types of hydrodynamic boundary conditions along the lateral edges of the channel. Lee [8] Carried a combined numerical and theoretical investigation of laminar natural convection heat and mass transfer in open vertical parallel plates with unheated entry and unheated exit is presented. Both boundary conditions of uniform wall temperature/uniform wall concentration (UWT/UWC) and uniform heat flux/uniform mass flux, (UHF/UMF) are considered. Results of dimensionless induced volume rate, average Nusselt number and Sherwood number are obtained for air flow under various buoyancy ratio, Grashof number, Schmidt number, and combinations of unheated entry, heated section and unheated exit length. Theoretical solutions for dimensionless induced volume rate, average Nusselt number and average Sherwood number for both UWT/UWC and UHF/UMF cases are derived under fully developed conditions. Mobedi and Sunden [9] investigated a steady state conjugate conduction-convection on vertical plate fin in which a small heat source is located. Heat from the fin surface is transferred to the surroundings by laminar natural convection. The governing equations for the problem are the heat conduction equation for the fin and the boundary layer equations, which are continuity, momentum and energy equations, for the fluid. A computer program is written by using the finite difference method in order to solve the governing equations which are nonlinear and coupled. The best location of the heat source in the fin for maximum heat transfer rate depends on two parameters which are the conduction-convection parameter and the Prandtl number. The obtained results have shown that for the fin with large conduction-convection parameter, a heat source location for maximum heat transfer rate exists. Levy *et al.* [10] addressed the problem of optimum plate spacing for laminar natural convection flow between two plates. Churchill, using the theoretical and

experimental results obtained by a number of authors for the mean rate of heat transfer in laminar buoyancy-driven flow through vertical channels, developed general correlation equations for these results.

Lewandowski and Radziemska [11] presented a theoretical solution of natural convective heat transfer from isothermal round plates mounted vertically in the unlimited space. With simplifying assumptions typical for natural heat transfer process, equations for the velocity profile in the boundary layer and the average velocity were obtained. Using this velocity, the energy flow within the boundary layer was balanced and compared with the energy transferred from the surface of the vertical plate according to the Newton's law. The solution of the resulting differential equation is presented in the form of a correlation between the dimensionless Nusselt and Rayleigh numbers. The theoretical result is compared with the correlation of numerical results obtained using Fluent software (Ansys Fluent 17.0). Experimental measurements of heat transfer from a heated round vertical plate 70 mm in diameter were performed in both water and air. The theoretical, numerical, and experimental results are all in good agreement. Dey *et al.* [12] found that the local flow field around a fin can substantially enhance the forced convection heat transfer from a conventional heat sink. A fin is set into oscillation leading to rupture of the thermal boundary layer developed on either side of the fin. This enhancement in heat transfer is demonstrated through an increase in the time-averaged Nusselt Number on the fin surfaces.

Awasarmol and Pise [13] reported that the perforated fin can enhance heat transfer. The magnitude of heat transfer enhancement depends upon angle of orientation, diameter of perforations and heater input. The perforation of fins enhances the heat dissipation rates and at the same time decreases the expenditure for fin materials. It helps making fin arrays light weight. Kundu and Wongwises [14] studied decomposition analysis on convecting-radiating rectangular plate fins for variable thermal conductivity and heat transfer coefficient. They concluded that the variable thermal conductivity did not make a significant role on the temperature and fin-wall performances in radiative and convective environment. Kundu and Lee [15] determined the minimum shape of porous fins with convection and radiation modes of heat transfer taken place on its surfaces. They proposed that optimum shape of porous fins as strong function with porosity. Singh and Patil [16] reported the heat dissipation ability of the naturally cooled heat sink has been found to increase by the application of impressions on

the fin body. Roul and Nayak [17] also studied experimentally the natural convection heat transfer from the internal surface of heated vertical tubes. Deshmukh and Warkhedkar [18] investigated the effects of design parameters of the fully shrouded elliptical pin fin heat sinks. On the basis of experimental measurements, the overall heat transfer coefficient and the thermal performance characteristics are obtained for various parameters with the inline and staggered layout of the pin fin heat sinks in mixed convection with assisting flow.

Taler [19] presented a numerical method for determining heat transfer coefficients in cross-flow heat exchangers with extended heat exchange surfaces. He used a nonlinear regression method to determine coefficients in the correlations defining heat transfer on the liquid and air-side. Correlation coefficients were determined from the condition that the sum of squared liquid and air temperature differences at the heat exchanger outlet, obtained by measurements and those calculated, achieved minimum. Minimum of the sum of the squares was found using the Levenberg-Marquardt method. The uncertainty in estimated parameters was determined using the error propagation rule by Gauss. The outlet temperature of the liquid and air leaving the heat exchanger was calculated using the analytical model of the heat exchanger.

Taler and Taler [20] presented different approaches for steady-state and transient analysis of temperature distribution and efficiency of continuous-plate fins. They suggested that for a constant heat transfer coefficient over the fin surface, the plate fin can be divided into imaginary rectangular or hexangular fins. They computed the transient temperature distributions in continuous fins attached to oval tubes using the finite volume methods. The developed method can be used in the transient analysis of compact heat exchangers to calculate accurately the heat flow transferred from the finned tubes to the fluid. Duda and Mazurkiewicz [21] presented the numerical modeling of steady state heat and mass transfer in cylindrical ducts for both laminar and hydro dynamically fully developed turbulent flow. Numerical results were compared with values obtained from analytical solution of such problems. The problems under consideration are often denoted as extended Graetz problems. Calculations were carried out gradually decreasing the mesh size in order to examine the convergence of numerical method to analytical solution.

When a vertical plate is heated a free-convection boundary layer is formed over the surface, as shown in Fig. 1. Inertial, viscous and buoyant

forces are predominant in this layer. The velocity profile in this boundary layer is quite unlike the velocity profile in a forced convection boundary layer. At the wall, the velocity is zero because of no-slip condition; it increases to some maximum value and then decreases to zero at the edge of the boundary layer since the free stream conditions are at rest in the free-convection system. The initial boundary layer development is laminar; however, at some distance from the leading edge, depending on the fluid properties and temperature to which the wall is subjected, turbulent eddies are formed, and transition to a turbulent boundary layer begins. After certain distance up the plate the boundary layer may become fully turbulent.

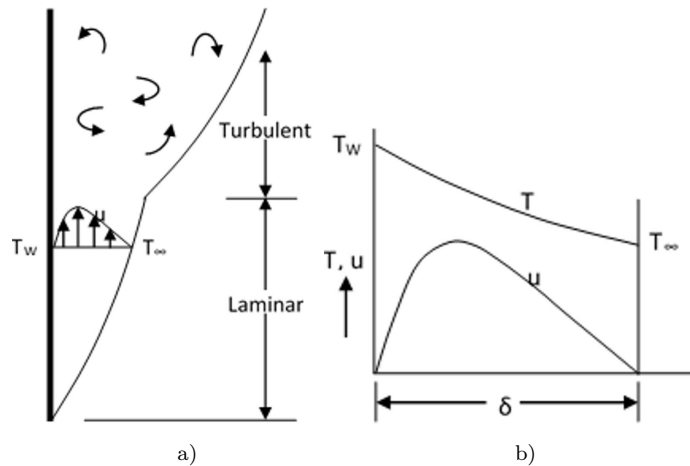


Figure 1: Boundary layer on a vertical flat plate (a), velocity and temperature distribution in the boundary (b).

Over the years it has been found that average free-convection heat transfer coefficients can be represented in the following functional form for a variety of circumstances:

$$\overline{Nu}_f = C (Gr_f Pr_f)^m, \quad (1)$$

where Gr and Pr are the Grashof and Prandtl numbers, respectively, C is the constant, and the exponent m is the empirical constant to be determined from experimental data, the subscript f indicates that the properties in the dimensionless groups are evaluated at the film temperature, which is given by

$$T_f = \frac{T_w + T_\infty}{2}, \quad (2)$$

where T_w and T_∞ are the wall and free-stream temperature, respectively.

The product of Grashof and Prandtl numbers is called the Rayleigh number

$$\text{Ra} = \text{GrPr} . \quad (3)$$

The characteristic dimensions used in the Nusselt and Grashof numbers depend on the geometry of the problem. For a vertical plate it is the height of the plate, whereas for a horizontal cylinder it is the diameter, and so forth. Experimental data for free convection problems appear in a number of references as given in the following paragraph.

For vertical surfaces, the Nusselt and Grashof numbers are formed with L , the height of the surface as the characteristic dimension. If the boundary layer thickness, δ , is not large compared to the diameter of the cylinder, the heat transfer may be calculated with the same relations used for vertical plates. The general criterion is that a vertical cylinder may be treated as a vertical flat plate [22], when

$$\frac{D}{L} \geq \frac{35}{\text{Gr}_L^{1/4}} , \quad (4)$$

where D is the diameter of the cylinder and Gr_L is the Grashof number for characteristic length L . For isothermal surfaces, the values of the constants are given by Vliet [22]. There are some indications from the analytical work of various investigators that the following relation may be preferable:

$$\text{Nu}_f = 0.10 (\text{Gr}_f \text{Pr}_f)^{1/3} . \quad (5)$$

More complete relations have been provided by Churchill and Chu [23] and are applicable over wider ranges of the Rayleigh number:

$$\overline{\text{Nu}} = 0.68 + \frac{0.670 \text{Ra}^{1/4}}{\left[1 + (0.492/\text{Pr})^{9/16}\right]^{4/9}} \quad \text{for } \text{Ra}_L < 10^9 , \quad (6)$$

$$\overline{\text{Nu}}^{1/2} = 0.825 + \frac{0.387 \text{Ra}^{1/6}}{\left[1 + (0.492/\text{Pr})^{9/16}\right]^{8/27}} \quad \text{for } 10^{-1} < \text{Ra}_L < 10^{12} , \quad (7)$$

where where overbar represents the average value and Ra_L is the Rayleigh number for characteristic length L . These equations are also a satisfactory representation for constant heat flux. Properties for these equations are

evaluated at the film temperature.

Extensive experiments have been reported in the literature for free convection from vertical and inclined surfaces to water under constant heat-flux conditions. In such experiments, the results are presented in terms of a modified Grashof number

$$\text{Gr}_x^* = \text{Gr}_x \text{Nu}_x = \frac{g\beta q_w x^4}{k\nu^2}, \quad (8)$$

where Gr_x and Nu_x are the Grashof and Nusselt numbers for characteristic length x , q_w is the wall heat flux, β is the coefficient of thermal expansion g is the gravitational acceleration, ν is the kinematic viscosity, and k is the thermal conductivity. The local heat transfer coefficients are correlated by the following relation for the laminar range:

$$\text{Nu}_{xf} = \frac{hx}{k_f} = 0.60 (\text{Gr}_x^* \text{Pr}_f)^{1/5} \quad \text{for} \quad 10^5 < G_x^* < 10^{11}. \quad (9)$$

For the turbulent region, the local heat-transfer coefficients are correlated with

$$\text{Nu}_x = 0.17 (\text{Gr}_x^* \text{Pr})^{1/4} \quad \text{for} \quad 2 \times 10^3 < \text{Gr}_x^* \text{Pr} < 10^{16}. \quad (10)$$

All properties in the above correlation are evaluated at the local film temperature. Although these experiments were conducted for water, the resulting correlations are shown to work for air as well. Rewriting Eq. (10) as a local heat transfer form gives

$$\text{Nu}_x = C (\text{Gr}_x \text{Pr})^m, \quad (11)$$

and substituting the value of Gr_x gives

$$\text{Nu}_x = C^{1/(1+m)} (\text{Gr}_x^* \text{Pr})^{1/(1+m)}. \quad (12)$$

The value of m for laminar and turbulent flow are taken as 1/4 and 1/3, respectively. Churchill and Chu [23] suggested that Eq. (6) may be modified to apply to the constant heat flux case if the average Nusselt number is based on the wall heat flux and the temperature difference at the center of the plate ($x = L/2$). The result is

$$\overline{\text{Nu}}_L^{1/4} [\overline{\text{Nu}}_L - 0.68] = \frac{0.67 (\text{Gr}_L^*)}{[1 + (0.492/\text{Pr})^{9/16}]^{4/9}}, \quad (13)$$

where $\overline{\text{Nu}}_L = q_w L / (k \overline{\Delta T})$ and $\overline{\Delta T} = T_w - T_\infty$, here $\overline{\text{Nu}}_L$ is the average Nusselt number for characteristic length L , which is based on the constant wall heat flux, and $\overline{\Delta T}$ is the difference of temperature between the wall and the fluid at the center of the plate, i.e., T_w is taken at $L/2$.

The purpose of this work is to study experimentally the natural convection heat transfer from the internal surface of heated vertical pipes at different heating levels. The test section is a vertical, open-ended cylindrical pipe dissipating heat from the internal surface. The test section is electrically heated imposing the circumferentially as well as axially constant wall heat flux. As a result of the heat transfer to air from the internal surface of the pipe, the temperature of air increases. As a result of which the density of air inside the pipe decreases which causes the air to rise. Although extensive work has been done on the study of natural convection heat transfer and hydrodynamics in heated vertical open-ended channels without internal rings, but the works on heat transfer from internal surfaces with presence of internal rings of different thicknesses are not adequate in literature.

Four different test sections and various uniform heat fluxes $q_w = \text{constant}$ were considered. Ratios of length, L , to diameter, D , of the test sections, for different channel length, were taken as $L/D = 10, 12.22, 15.56,$ and 18.89 . In the case of channels with internal discrete rings, of rectangular section, placed at various distances, the dimension ratios were taken as: ratios of ring thickness, t , and step size, s , to diameter $t/D = 0.089\text{--}0.178$ and $s/D = 1.67\text{--}6.29$, respectively and ratio $s/t = 9.375\text{--}70.82$.

2 Experimental set-up and procedure

The experimental set-up consists of a test section, electrical circuit for heating and a measuring system as shown in Fig. 2. The cross-sectional view of the test section is shown in Fig. 3. In this study, a hollow tube is made of aluminium which is 45 mm in diameter and 3.8 mm thick. Nine copper-constantan thermocouples are fixed to monitor temperatures on the internal surface at various locations as shown in the figure. Holes of 0.8 mm diameter are drilled at these locations for inserting the thermocouples. After inserting the thermocouple junction, the holes are filled with aluminium powder for getting good thermal contact with the tube. Then the openings of the thermocouple wells are closed by punching with a dot punch. Epoxy is used for sealing the opening of the thermocouple wells and for holding

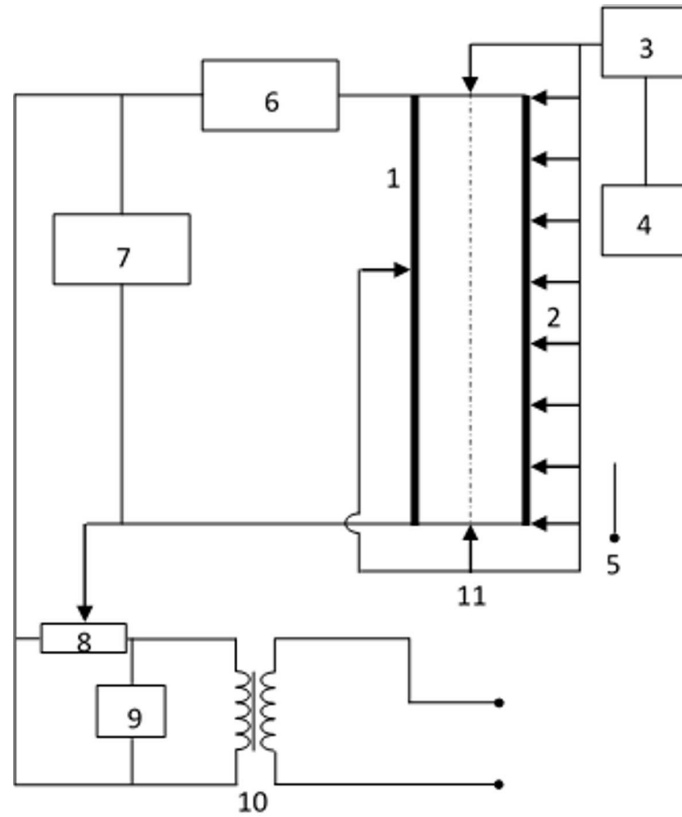


Figure 2: Experimental set-up: 1 – test section, 2 – system of thermocouples, 3 – selector switch, 4 – millivoltmeter, 5 – thermometer, 6 – ammeter, 7 – and 9 – voltmeter, 8 – variable transformer, 10 – transformer, 11 – traversing type thermocouples.

the thermocouples in position.

After mounting the thermocouples, a layer of asbestos paste (10 mm thick) is provided on the outer surface of the tube. A layer of glass tape is provided over the asbestos paste and then the nichrome wire heater coil is helically wound around the external surface with equal spacing. Then asbestos rope of diameter approximately 7 mm is wound over the heater coil with close fitting. After that another layer of asbestos paste is provided. A layer of glass-fibers of approximately 15 mm thickness is wrapped around it. A thick cotton cloth is wrapped over the glass fibers. It is covered with a very thin aluminium foil for reducing the radiation heat transfer. Two traversing type thermocouples are provided; one at the entrance and the

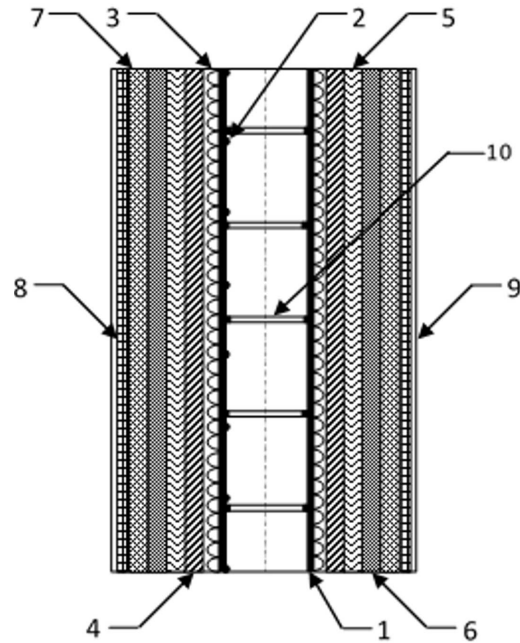


Figure 3: Cross-sectional view of the test section: 1 – aluminium tube, 2 – position of thermocouples, 3 – heater coil, 4 – glass tape, 5 – asbestos rope, 6 – asbestos paste, 7 – glass fibre, 8 – cotton cloth, 9 – aluminium foil, 10 – internal rings.

other at the exit, to determine the temperature profile of fluid entering and leaving the tube at different radial distances. Another traversing type thermocouple is also used for measuring the external surface temperature of the test section to find out the heat loss from the external surface.

Wall temperatures at different locations are found out from the millivoltmeter readings to which thermocouples are connected. The fluid temperatures at the channel exit and entrance are found out at various radial distances by two traversing type thermocouples provided at the top and bottom of the channel, respectively. The electric power input to the test section is determined from the measured voltage drop across the test section and the current along the test section.

Though adequate thermal insulation is provided on the outer surface of the tube, there is still some heat rejection from the external surface and this heat loss by natural convection from the test section through the insulation is evaluated by measuring the outer surface temperature of the insulation and the ambient temperature. At different axial locations along the pipe

the outer surface temperature of the insulator are measured by thermocouples and the average insulation temperature is determined. Heat loss from the external surface is then computed by the suggested correlation [24] for natural convection from a vertical cylinder in air. Now heat dissipated from the internal surface can be found out by subtracting this heat loss from the heat input to the test section. The wall heat flux, q_w , can be found out by dividing this heat by the internal surface area. From the measured temperature profiles at the channel entrance and exit, the approximate temperature profile at any other axial distance can be calculated.

Let the local wall temperatures at different axial distance along the pipe be T_{w1} , T_{w2} , T_{w3}, \dots , and the bulk temperature (the temperature of the fluid "far" from the wall) at these distances be T_{b1} , T_{b2} , T_{b3}, \dots , respectively, then local heat transfer coefficient at these locations can be calculated by the relation

$$h_1 = \frac{q_w}{(T_{w1} - T_{b1})}, \quad (14)$$

similarly h_2, h_3, h_4, \dots can be calculated from which average heat transfer coefficient \bar{h} is found. The average Nusselt number can be found from the average heat transfer coefficient by using the relation

$$\overline{\text{Nu}} = \frac{\bar{h}D}{k}. \quad (15)$$

Now modified Rayleigh number based on constant heat flux and average wall temperature can be calculated by using the following formulas:

$$\text{Ra}^* = \text{Gr Pr} \frac{D}{L} = \frac{g\beta q_w D^5}{\alpha \nu k L}, \quad (16)$$

$$\text{Ra}^* = \frac{g\rho^2 c_p \beta (\overline{T_w} - \overline{T_b}) D^4}{Lk\mu}, \quad (17)$$

where α is the thermal diffusivity, c_p is the specific heat capacity at constant pressure, and μ is the dynamic viscosity.

A vane type anemometer [25] is used to measure the velocity of fluid at the exit of the channel. The modified Reynolds number can be calculated by using the relation:

$$\text{Re}^* = \frac{\bar{u}D^2}{\nu L}. \quad (18)$$

Experiments were conducted on four different test sections having 45 mm internal diameter, D , and 3.8 mm thickness. The length of the test sections, L , were 450 mm, 550 mm, 700 mm, and 850 mm, respectively. Hence, the ratios of length to diameter of the test sections were taken as $L/D = 10, 12.22, 15.56, \text{ and } 18.89$. Similarly studies were also carried out on channels, of the same geometrical sizes, with internal rings of rectangular section placed at various distances. Thickness of the rings were taken as $t = 4 \text{ mm}, 6 \text{ mm}, 8 \text{ mm}$, and the step size, s , of the rings was varied from 75 mm to 283.3 mm, therefore, the other ratios were taken as: $s/D = 1.67\text{--}6.29$, $t/D = 0.089\text{--}0.178$, and $s/t = 9.375\text{--}70.82$.

For each test section experiments were conducted for eight different heat flux values. Since the wall temperature was difficult to be maintained constant, only the uniform wall heat flux case, $q_w = \text{constant}$, was considered, and wall heat fluxes were maintained at $q_w = 250\text{--}3341 \text{ W/m}^2$. Total 320 numbers of experiments were conducted and to perform each experiment around 4 hours were required for steady state conditions to be reached. Even after 4 hours, it was very difficult to obtain steady state condition. So, a number of observations were taken for each experiment and average data was reported. This average value was found to have deviations within $\pm 2\%$.

As the results of the study, spatial variations of the local wall temperatures as well as temperature profiles at the channel exit were plotted for the smooth channel and the channel provided with various discrete rings for different heat fluxes and channel length.

3 Results and discussion

Figure 4a and 4b illustrate the typical axial variations of local wall temperatures for various L/D ratios and for various heat fluxes for smooth tubes. It can be seen from these figures that the wall temperature increases along the height of the cylinder, which is in accordance with the theoretical predictions done by various investigators. But it slightly decreases towards the end, which may be due to the heat rejection from the end of the tubes as the thickness of the tube is not negligible.

Experimental temperature profiles at the channel exit for different heat fluxes and for different L/D ratio for smooth tubes are indicated in Fig. 5a,b. The radial distances are taken as abscissa whereas the fluid temperatures

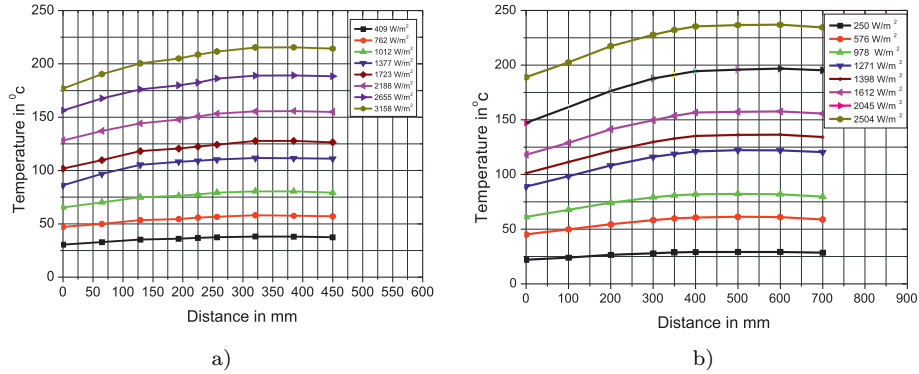


Figure 4: Variation of wall temperature for different heat fluxes and channel lengths: a) $L = 450$ mm, b) $L = 700$ mm.

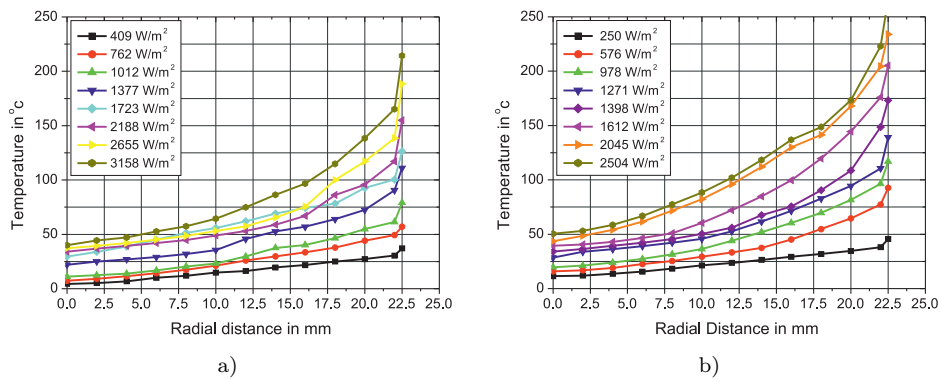


Figure 5: Temperature profile at channel exit for different wall heat fluxes and channel lengths for smooth tubes: a) $L = 450$ mm, b) $L = 700$ mm.

are taken as the ordinate. Here the distances are measured from the center of the pipe towards the wall at the exit of the test section. The radial distance at the center equals zero and at the wall is equal to $D/2 = 22.5$ mm. It is evident from these figures that the fluid temperature is maximum at the wall which is nearly equal to the wall temperature at the exit of the pipe and it minimum at the center of the pipe. This is due to the fact that heat is transferred from the wall of the heated pipe to the air by natural convection. So, the air in the vicinity of the wall is hotter as compared to the air farther the wall.

Similarly, studies are also carried out on intensified channels of the

same geometrical sizes by providing internal rings of same material of different thickness, t placed at various distances with step size, s . The non-dimensional ratios are taken as: $s/D = 1.67\text{--}6.29$, $t/D = 0.089\text{--}0.178$ and $s/t = 9.375\text{--}70.82$. Experimental temperature profiles at the channel exit for different heat fluxes and for different L/D ratio for tubes with internal rings are indicated in Figs. 6a to 6k. It is evident from these figures that the fluid temperature is maximum at the wall which is nearly equal to the wall temperature and minimum at the center of the pipe. It can also be seen from these figures that the air temperature at the center of the pipe is more in case of pipes with internal rings as compared to that of smooth pipes. This is due to the fact that there is enhancement of heat transfer from the wall to the air when internal rings are provided. As hot layers diffuse to the center of flow, and the cold ones move to wall area, the gradient of temperature in the boundary layer increases, and thus heat transfer increases.

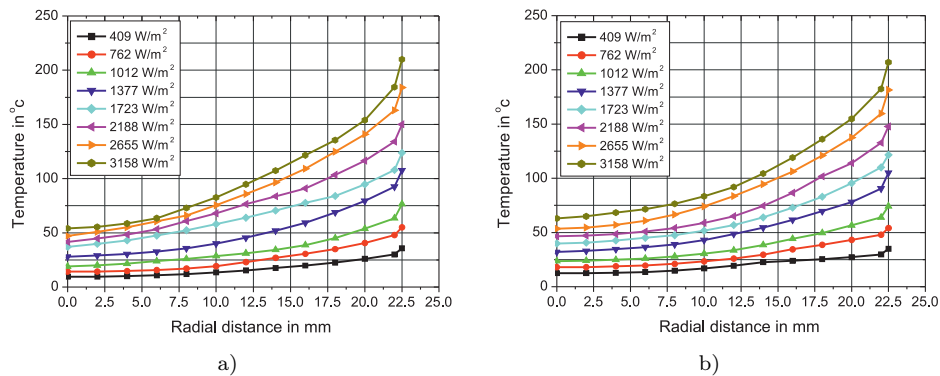
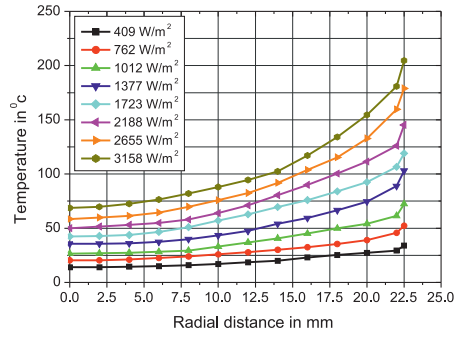
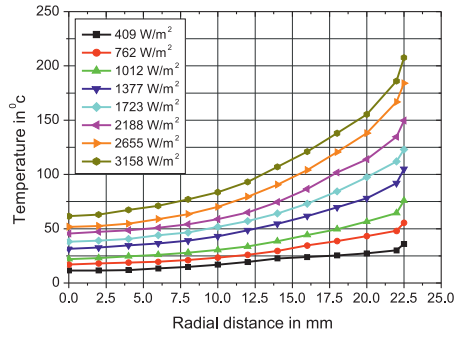


Figure 6: a) and b). For caption see page 103.

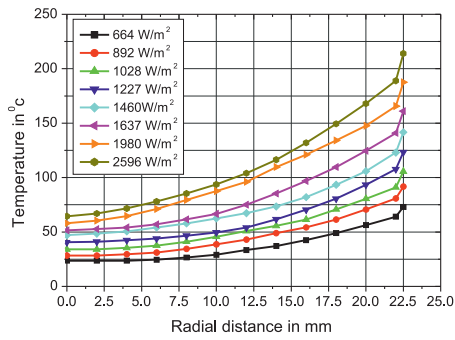
It can also be seen that the average heat transfer rate increases with increasing the thickness of the rings up to a certain limit, beyond which it decreases. When ring thickness increases from 4 mm to 6 mm there is enhancement of heat transfer from the wall to air. But by further increasing the ring thickness from 6 mm to 8 mm there is slight decrease in heat transfer. This may be due to the fact that when the ring thickness increases, the intensity of pulsation will increase and the pulsation arising behind the ring will have no time to fade sufficiently on the way to the following ring and will diffuse to the flow core. Thus intensity of pulsation will increase and consequently the turbulence of flow will occur. This results in significant



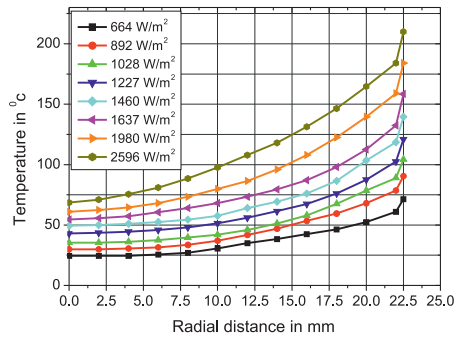
c)



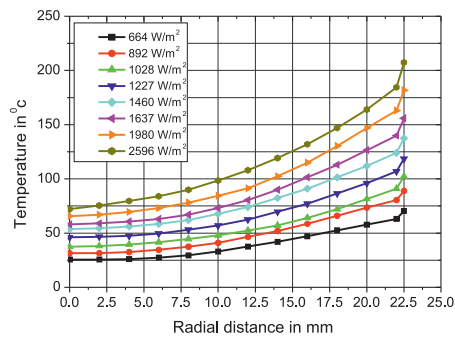
d)



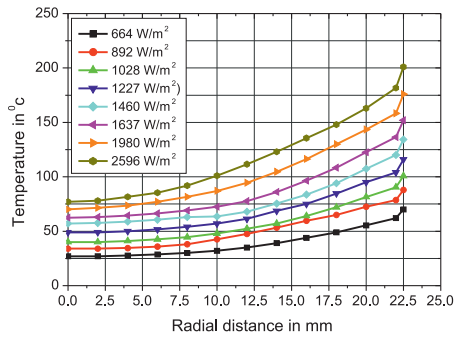
e)



f)



g)



h)

Figure 6: c)–h). For caption see page 103.

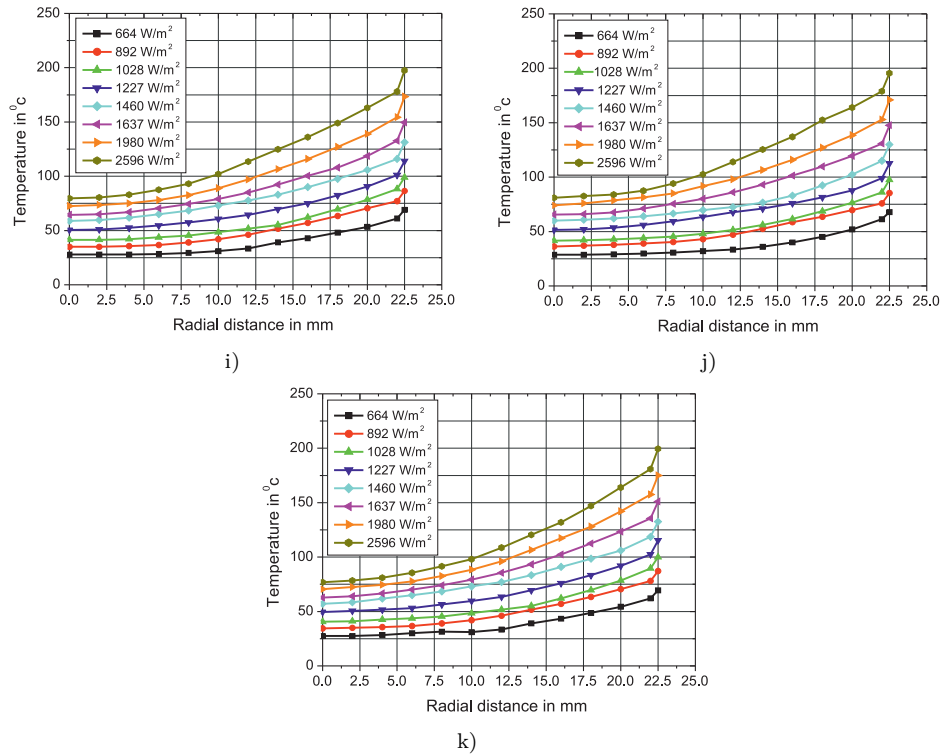


Figure 6: Distribution of temperature of flow at the exit of the tube with internal rings: a) $L/D = 10$, $t = 6$ mm, $s = 250$ mm; b) $L/D = 10$, $t = 6$ mm, $s = 150$ mm; c) $L/D = 10$, $t = 6$ mm, $s = 112.5$ mm; d) $L/D = 10$, $t = 6$ mm, $s = 75$ mm; e) $L/D = 18.89$, $t = 4$ mm, $s = 425$ mm; f) $L/D = 18.89$, $t = 4$ mm, $s = 283.33$ mm; g) $L/D = 18.89$, $t = 4$ mm, $s = 212.5$ mm; h) $L/D = 18.89$, $t = 6$ mm, $s = 425$ mm; i) $L/D = 18.89$, $t = 6$ mm, $s = 283.33$ mm; j) $L/D = 18.89$, $t = 6$ mm, $s = 212.5$ mm; k) $L/D = 18.89$, $t = 8$ mm, $s = 212.5$ mm.

growth of hydraulic resistance with small increase of heat transfer.

Figure 7 shows the distribution of temperatures of flow at outlet of channels for various L/D ratio, i.e., for different length of the tube. It is clear from the graph that heat transfer increases with increase in tube length. This is because by increasing the length of the test sections the surface area increases as a result of which the heat transfer from the wall to air increases.

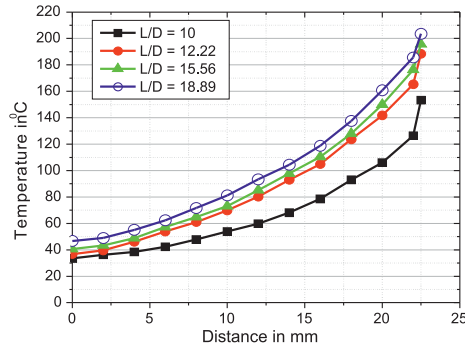


Figure 7: Temperature profiles at the channel exit for smooth tubes with different length.

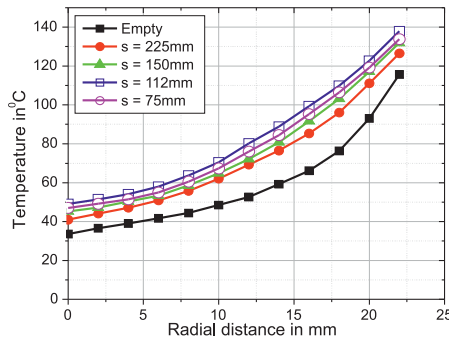


Figure 8: Temperature profiles at the channel exit for tubes with discrete rings.

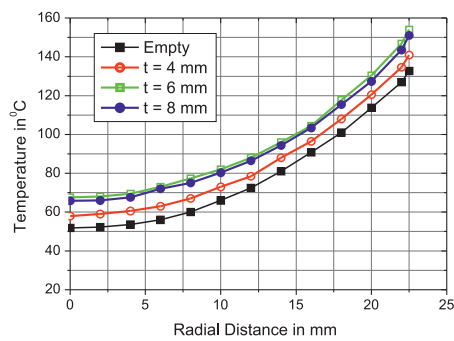


Figure 9: Temperature profiles at the channel exit for different ring spacing.

Figures 8 and 9 show the distributions of temperature of flow at outlet of channels for various heat fluxes and various thickness and spacing of rings inside the tube. It can be seen that the average heat transfer rate increases with increasing the thickness of the rings up to a certain limit, beyond which it decreases, which is shown in Fig. 9. Figure 8 shows that when the spacing between the rings decreases beyond a certain limit, the heat transfer rate decreases. This may be due to the fact that with an often arrangement of rings the pulsation arising behind the ring will have no time to fade sufficiently on the way to the following ring and will defuse to the flow core. Thus, intensity of pulsation will increase and consequently the turbulence of flow will occur. This results in significant growth of hydraulic resistance with small increase of heat transfer.

3.1 Relationship between Nusselt number and Rayleigh number

Figure 10 shows the relationship between the experimentally obtained average Nusselt number and modified Rayleigh number, which is plotted on log-log scale. A correlation between average Nuusselt number and modified Rayleigh number for laminar natural convection in smooth vertical tubes has been developed as

$$\overline{Nu} = 0.33 \times (Ra)^{0.31} . \tag{19}$$

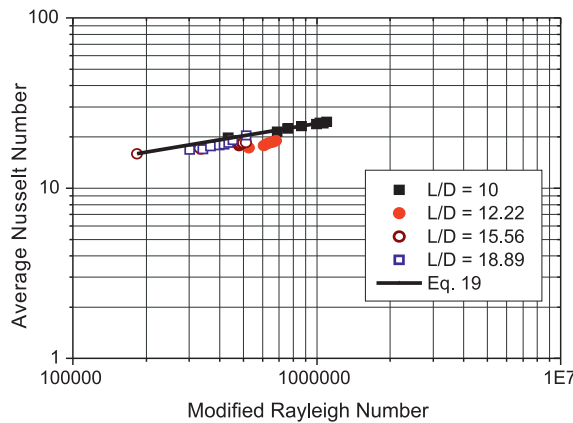


Figure 10: Relationships between the experimentally obtained average Nusselt number and modified Rayleigh number.

3.2 Relationship between Reynolds number and Rayleigh number

Figure 11 shows the relationship between experimentally obtained modified Reynolds number and modified Rayleigh number, which are plotted on the logarithmic scale. This correlation can be obtained as

$$Re^* = 0.49 \times (Ra^*)^{1/3} . \tag{20}$$

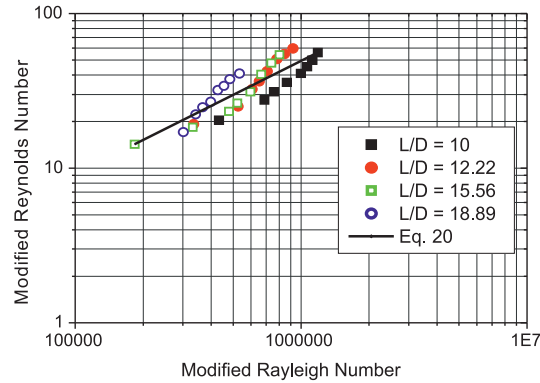


Figure 11: Relationship between experimentally obtained modified Reynolds number and modified Rayleigh number.

4 Conclusions

Experimental investigation of natural convection heat transfer in a vertical pipe has been conducted both for smooth pipes and for pipes with internal rings. The effects of channel length, wall heat flux, ring thickness, and ring spacing on the characteristics of natural convection heat transfer are examined in detail. The following conclusions have been drawn from the present investigation:

1. Average heat transfer rate from the internal surfaces of a heated vertical pipe increases with increase in length of the test section.
2. Average heat transfer rate from the internal surfaces of a heated vertical pipe increases discrete rings are provided.
3. Average heat transfer rate increases with increasing the thickness of the rings up to certain value, beyond which it decreases.
4. Average heat transfer rate increases with increasing the number of rings i.e. reducing the spacing between the rings up to a certain value of spacing, but further reduction in ring spacing, reduces the heat transfer rate from the internal wall to air.
5. A correlation between average Nusselt number and modified Rayleigh number was proposed as given in Eq. (19), which can predict the data accurately within $\pm 5\%$ error.

6. Another correlation between modified Rayleigh number and modified Reynolds number was proposed as given in Eq. (20), which can predict the data within $\pm 10\%$ error.

Received 16 April 2017

References

- [1] IYI D., HASAN R.: *Natural convection flow and heat transfer in an enclosure containing staggered arrangement of blockages*. Procedia Engineering **105**(2015), 176–183.
- [2] BUONOMO B., MANCA O.: *Transient natural convection in a vertical micro channel heated at uniform heat flux*. Int. J. Thermal Sciences **56**(2012), 35–47.
- [3] MALIK S.K., SASTRI, V. M. K.: *Experimental investigation of natural convection heat transfer over an array of staggered discrete vertical plates*. J. Energy Heat and Mass Transfer **18**(1996), 127–133.
- [4] HUANG G.J., WONG S.C., LIN C.P.: *Enhancement of natural convection heat transfer from horizontal rectangular fin arrays with perforations in fin base*. Int. J. Thermal Sciences **84**(2014), 164–174.
- [5] CHENG C.Y.: *Fully developed natural convection heat and mass transfer in a vertical annular porous medium with asymmetric wall temperatures and concentrations*. Appl. Therm. Eng. **26**(2006), 2442–2447.
- [6] CAPOBIANCHI M., AZIZ A.: *A scale analysis for natural convective flows over vertical surfaces*. Int. J. Therm. Sci. **54**(2012), 82–88.
- [7] SPARROW E. M., BAHRAMI P.A.: *Experiments in natural convection from vertical parallel plates with either open or closed edges*. J. Heat Trans-T. ASME **102**(1980), 221–227.
- [8] LEE K.T.: *Natural convection heat and mass transfer in partially heated vertical parallel plates*. Int. J. Heat Mass Tran. **42**(1999), 4417–4425.
- [9] MOBEDI M., SUNDEN B.: *Natural convection heat transfer from a thermal heat source located in a vertical plate fin*. Int. Commun. Heat Mass **33**(2006), 943–950.
- [10] LEVY E. K., EICHEN P.A., CINTANI W.R., AND SHAW R.R.: *Optimum plate spacing for laminar natural convection heat transfer from parallel vertical isothermal flat plates: experimental verification*. J. Heat Transfer-T ASME **97**(1975), 474–476.
- [11] LEWANDOWSKI W.M., RADZIEMSKA E.: *Heat transfer by free convection from an isothermal vertical round plate in unlimited space*. Appl. Energ. **68**(2001), 187–201.
- [12] DEY S., CHAKRABORTY D.: *Enhancement of convective cooling using oscillating fins*. Int. Commun. Heat Mass **36**(2009), 508–512.
- [13] AWASARMOL U. V., PISE A. T.: *An experimental investigation of natural convection heat transfer enhancement from perforated rectangular fins array at different inclinations*. Exp. Therm. Fluid Sci. **68**(2015), 145–154.

- [14] KUNDU B., WONGWISES S.: *Decomposition analysis on convecting– radiating rectangular plate fins for variable thermal conductivity and heat transfer coefficient*. J. Franklin Inst. **349**(2012), 966–984.
- [15] KUNDU B., LEE K.S.: *Exact analysis for minimum shape of porous fins under convection and radiation heat exchange with surrounding*. Int. J. Heat Mass Transfer **81**(2015), 439–448.
- [16] SINGH P., PATIL A.K.: *Experimental investigation of heat transfer enhancement through embossed fin heat sink under natural convection*. Exp. Therm. Fluid Sci. **61**(2015), 24–33.
- [17] ROUL M.K., NAYAK R.C.: *Experimental investigation of natural convection heat transfer through heated vertical tubes*. Int. J. Engineering Research and Applications **2**(2012), 1088–1096.
- [18] DESHMUKH P.A., WARKHEDKAR R.M.: *Thermal performance of elliptical pin fin heat sink under combined natural and forced convection*. Exp. Thermal Fluid Sci. **50**(2013), 61–68.
- [19] TALER D.: *Experimental determination of correlations for mean heat transfer coefficients in plate fin and tube heat exchangers*. Arch. Thermodyn. **33**(2012), 1–24.
- [20] TALER D., TALER J.: *Steady-state and transient heat transfer through fins of complex geometry*. Arch. Thermodyn. **35**(2014), 117–133.
- [21] DUDA P., MAZURKIEWICZ G.: *Numerical modeling of heat and mass transfer in cylindrical ducts*. Arch. Thermodyn. **31**(2010), 33–43.
- [22] VLIET G.C.: *Natural convection local heat transfer on constant-heat-flux inclined surfaces*. J. Heat Transfer **91**(1969), 4, 511–516.
- [23] CHURCHILL S.W., CHU H.H.S.: *Correlating equations for laminar and turbulent free convection from a vertical plate*. Int. J. Heat Mass Transfer **18**(1975), 1323–1329.
- [24] HOLMAN J.P.: *Heat Transfer*. McGraw-Hill, Tenth Edition 2010.
- [25] VELMURUGAN P., KALAIVANAN R.: *Energy and exergy analysis in double-pass solar air heater*. Sadhana **41**(2016), 369–376.

Appendix

Sample calculations for $q_w = 2188 \text{ W/m}^2$, $L = 0.450 \text{ m}$, $L/D = 10$, and $D_1 = 0.12 \text{ m}$, where D_1 denotes the external diameter of the test section.

A Heat loss from external surface

Average surface temperature excess over ambient: $\Delta T = 18 \text{ K}$, $T_\infty = 300 \text{ K}$.

Average temperature of fluid (film temperature): $T_f = 300 + 18/2 = 309 \text{ K}$.

The different property values of air at one atm (0.101325 MPa). Pressure can be found out from the data table as follows:

$$\beta = \frac{1}{T_f} = \frac{1}{309 \text{ K}} = 3.236 \times 10^{-3} \frac{1}{\text{K}},$$

$$\begin{aligned} \text{Ra} &= \text{Gr Pr} = \frac{g\beta(T_w - T_\infty)D_1^3}{\nu^2} \times \text{Pr} \\ &= \frac{9.81 \text{ m/s}^2 \times 3.236 \times 10^{-3} \text{ 1/K} \times 18 \text{ K} \times (0.12 \text{ m})^3}{(16.576 \times 10^{-6} \text{ m}^2/\text{s})^2} \times 0.6998 \\ &= 2.515 \times 10^6, \end{aligned}$$

$$\overline{\text{Nu}}^{\frac{1}{2}} = 0.825 + \frac{0.387 \text{ Ra}^{\frac{1}{6}}}{\left[1 + \left(\frac{0.494}{\text{Pr}}\right)^{\frac{9}{16}}\right]^{\frac{8}{27}}} = 4.604,$$

$$\overline{\text{Nu}} = 21.198,$$

and finally

$$\bar{h} = \frac{\overline{\text{Nu}}k}{D_1} = \frac{21.198 \times 0.027236 \text{ W/m K}}{0.12 \text{ m}} = 4.811 \text{ W/m}^2\text{K}.$$

Heat lost from the external surface is

$$\begin{aligned} q_2 &= \bar{h} \times \pi \times D_1 \times L \times \Delta T \\ &= 4.811 \text{ W/m}^2\text{K} \times 3.14 \times 0.12 \text{ m} \times 0.45 \text{ m} \times 18 \text{ K} = 14.69 \text{ W}. \end{aligned}$$

B Wall heat flux

Heat input: $q_1 = 90 \text{ V} \times 1.71 \text{ A} = 153.9 \text{ W}$, (where 90 V and 1.71 A are the potential difference and current, respectively).

Heat rejected from the internal surface:

$$\begin{aligned} q &= q_1 - q_2 \\ &= 153.9 \text{ W} - 14.69 \text{ W} = 139.21 \text{ W}. \end{aligned}$$

Wall heat flux:

$$\begin{aligned} q_w &= \frac{q}{A} \\ &= \frac{139.21 \text{ W}}{3.14 \times 0.045 \text{ m} \times 0.45 \text{ m}} = 2188 \text{ W/m}^2, \end{aligned}$$

where $A = \pi \times D \times L$ is the internal surface area of test section.

C Heat transfer coefficient

The local heat transfer coefficient calculated at 8 different axial locations is presented in a tabular form as given in Tab. 1:

Table 1:

Thermocouple positions	Local wall temp. excess over ambient	Fluid temp. excess over ambient	$h = \frac{q_w}{(T_{wi} - T_{bi})}, (i = 1, \dots, 8)$
mm	K	K	W/m ² K
0	128.1	0.0	17.0800
65	137.2	5.0	16.5500
129	144.2	9.5	16.2440
193	147.8	14.0	16.3530
257	153.3	18.0	16.1700
321	155.5	23.5	16.5757
385	155.8	28.5	17.1877
450	155.0	34.0	18.0830

Consequently, the average wall and bulk temperatures, and average heat transfer coefficient are as follows:

$$\begin{aligned}\overline{T_w} &= 147.52 \text{ K} , \\ \overline{T_b} &= 17 \text{ K} , \\ \overline{h} &= \frac{134.243}{8} = 16.78 \text{ W/m}^2 \text{ K} .\end{aligned}$$

D Different dimensionless numbers:

$$T_f = T_\infty + \frac{\overline{T_w} - \overline{T_b}}{2} = 300 \text{ K} + \frac{420.52 \text{ K} - 290 \text{ K}}{2} = 365.26 \text{ K} .$$

The properties of air corresponding to this temperature are:

$$\begin{aligned}\nu &= 22.3328 \times 10^{-6} \text{ m}^2/\text{s} , \\ \alpha &= 32.2845 \times 10^{-6} \text{ m}^2/\text{s} , \\ k &= 0.031465 \text{ W/m K} , \\ \beta &= \frac{1}{365.26 \text{ K}} = 2.7378 \times 10^{-3} \frac{1}{\text{K}} .\end{aligned}$$

Average Nusselt Number:

$$\overline{Nu} = \frac{\overline{h}D}{k} = \frac{16.78 \text{ W/m}^2\text{K} \times 0.045 \text{ m}}{0.031465 \text{ W/m K}} = 23.998 .$$

Modified Rayleigh number:

$$\begin{aligned} Ra &= \frac{g\beta q_w D^5}{\alpha\nu k L} \\ &= \frac{9.81 \text{ m/s}^2 \times 2.7378 \times 10^{-3} \text{ 1/K} \times 2188 \text{ W/m}^2 \times (0.045 \text{ m})^5}{22.3328 \times 10^{-6} \text{ m}^2/\text{s} \times 32.2845 \times 10^{-6} \text{ m}^2/\text{s} \times 0.031465 \text{ W/m K} \times 0.45 \text{ m}} \\ &= 1.062182 \times 10^6 . \end{aligned}$$

Mean stream velocity: $\bar{u} = 0.225 \text{ m/s}$.

Modified Reynolds number:

$$Re = \frac{\bar{u}D^2}{\nu L} = \frac{0.225 \text{ m/s} \times (0.045 \text{ m})^2}{22.3328 \times 10^{-6} \text{ m}^2/\text{s} \times 0.45 \text{ m}} = 45.337 .$$